Front. Phys. 13(6), 132104 (2018)
https://doi.org/10.1007/s11467-018-0834-7

PERSPECTIVE

Approaching nuclei through multiple perspectives and diverse models: Patterns, symmetries, interactions

R. F. Casten[1,2]

[1] *Wright Nuclear Structure Laboratory, Yale University, New Haven, CT 06520, USA*
[2] *Michigan State University- FRIB, East Lansing, MI, USA*
E-mail: richard.casten@yale.edu
Received July 18, 2018; accepted July 29, 2018

Nuclei are complex objects yet display remarkable simplicities and regular patterns. The study of these and their origins has long been one of the twin pillars of nuclear structure research. We will discuss the behavior of atomic nuclei from this point of view. A key element will be the advantages of looking at the same data from different perspectives and of inter-relating these perspectives.

Keywords nuclear structure, simple patterns and symmetries, diverse perspectives and models, emergence of collectivity, residual interactions

PACS numbers 21.60.Cs, 21.10.Dr, 21.60.Ev, 21.30.Fe

1 Introduction

Nuclei are incredibly complex objects, consisting, at the nucleonic level, of up to hundreds of particles with structure dominated by both the strong and electromagnetic interactions. In a non-rigorous but informative way, the nucleons occupy about 60% of the nuclear volume and orbit $\sim 10^{21}$ times per second. One would expect utter confusion and chaos. However, remarkably, due largely to the short range and attractive nature of the nuclear force and to the Pauli and Heisenberg Principles, nuclei display astonishing simplicities of behavior and regular patterns. This has led, over the last decades, to two overarching approaches to nuclear structure which can colloquially be called the microscopic (in terms of nucleons and their interactions) and macroscopic (in terms of shapes and symmetries). This dual approach has been highlighted in numerous Long Range Plans and major institutional (e.g., U.S. National Academy) reports worldwide since the 1980s. The microscopic approach has grown tremendously in the last 15 years due to remarkable advances in the computing power needed for it. The more phenomenological shape/symmetry approach is complementary and provides deep insights into the structure of nuclei in an elegant and very intuitive way.

In this paper, we will focus primarily on the latter approach and, in particular, on the value of looking at nuclear data from diverse perspectives. A pivotal inspiration to look at nuclei in this way underlying much of the paper lies in the Interacting Boson Approximation (IBA) Model originally promulgated by Arima and Iachello in the mid-1970s [1–5], complemented by the contemporary work of Janssen, Jolos, and Donau [6], and the subject of almost countless studies since then. Many of the ideas presented here have been discussed or motivated by the presentation in Ref. [7].

2 Patterns and perspectives

Perhaps no figure illustrates the exceptionally simple patterns exhibited by atomic nuclei better than Fig. 1 which simply shows the empirical values (color coded) of the two basic observables, $E(2_1^+)$, the energy of the first excited 2^+ state in even-even nuclei, and $R_{4/2} = E(4_1^+)/E(2_1^+)$ which is typically <2 in non-collective nuclei near closed shells, ~2–2.3 in vibrational nuclei, near 2.5–2.7 in either transitional or gamma-soft nuclei and 3.33 in ideal deformed rotor nuclei. The figure outlines by thin horizontal and vertical lines the traditional magic numbers 20, 28, 40 (for protons), 50, 82, and 126.

In light of the above-mentioned complexity of the nuclear interior, the patterns displayed are remarkably sim-

*Special Topic: Simplicity, Symmetry, and Beauty of Atomic Nuclei (Eds. Jie Meng, Takaharu Otsuka & Yu-Min Zhao).

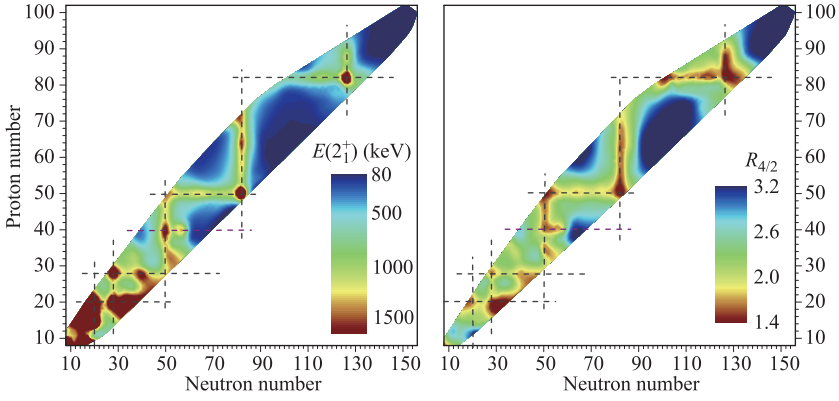

Fig. 1 Color coded display of $E(2_1^+)$ and $R_{4/2}$ across most of the nuclear chart. The traditional magic numbers are indicated by dashed lines. Figure courtesy of R. Burcu Cakirli.

ple, repetitive and elegant. Incidentally, the blurring and smearing of the boundaries of different colors in light nuclei reflects one of the major realizations of recent years, as studies of exotic, unstable nuclei have proliferated and advanced in power and sophistication, namely that the magic numbers, originally derived from data on accessible nuclei near stability, are actually fragile constructs which evolve (appear, disappear, soften) in nuclei far off stability. Research in exotic nuclei is the new frontier of nuclear structure studies, more and more linked to understanding nuclear reactions as well. It is made possible by a number of advanced facilities worldwide, with FRIB at MSU being the major, new, flagship, facility that will come on line in the next few years. These facilities are ushering in a revolution in our access to, and understanding of, nuclear structure and its drivers.

Inspired by this figure, we will spend the rest of this section looking at other patterns and regularities in nuclei, often guided by the value of looking globally at nuclear data from complementary perspectives.

To start we consider $R_{4/2}$ in a different way. In looking at a given region, say, the rare earth region from $Z \sim 50$–82 and $N \sim 82$–126, one often encounters plots of $R_{4/2}$ against neutron number, N. This is shown in Fig. 2(a). Clearly it shows the evolution from near closed shell nuclei, through a vibrator structure to well-deformed rotational nuclei. But, without delving into the details of the individual curves and their subtle crossings, it is hard to see more than this. However, exploiting the theme of looking at data from different perspectives, Fig. 2(b), which plots the *same* data but against Z, one sees a much richer diagnostic. Here the data points are connected according to their neutron number. One sees two sets of curves, concave for $N < 90$ and convex for $N \geq 90$. Recalling the $R_{4/2}$ is minimal near closed shells and maximal in deformed nuclei, this figure shows that:

- For $N < 90$, $Z = 64$ acts as a kind of magic number (microscopically this is well known as reflecting the gap between the $g_{7/2}$ and $d_{5/2}$ orbits, which can hold 14 nucleons, and the $h_{11/2}$ orbit). For $N = 90$ and above, the proton number $Z = 64$ is seen to be near mid-shell. So the figure shows that $Z = 64$ dissolves as a magic number near $N = 90$.
- At the same time, the qualitative change from concave to convex curves shows that this is a sudden break in behavior signaling a shape/phase transition at $N = 88$–90. Indeed, ^{152}Sm with 90 neutrons is the first and iconic example [9] of a near-X(5) nucleus [10] described by a first order quantum phase transition.
- Since the change in proton sub-shell character occurs as a function of neutron number this points to the valence p-n interaction as the mediator of changing proton shell structure via the monopole component of the interaction, which has the property of altering single particle energies.

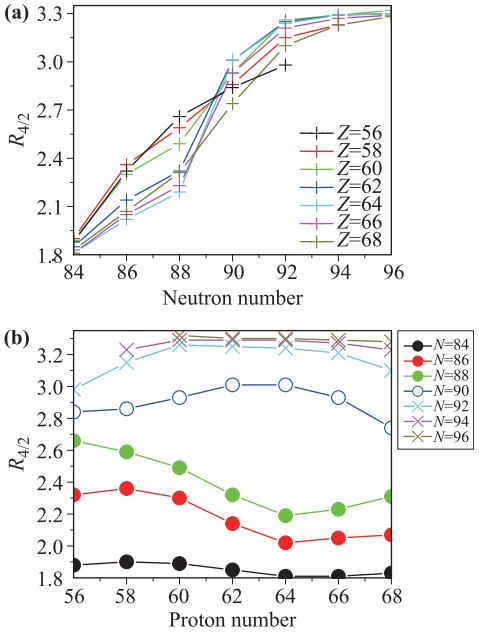

Fig. 2 $R_{4/2}$ against N **(a)** and Z **(b)** for the rare earth region showing different perspectives on structural evolution. Based on Ref. [8].

So, the lower panel actually shows that the onset of deformation occurs as a phase transition due to a change in proton shell closure as a function of neutron number mediated by the monopole p-n interaction. In principle, the same information can be (must be able to be) extractable from the top panel, but not easily, not intuitively, and, in practice, not.

Another example of looking at data from different perspectives is given in Fig. 3. Figure 3(a) shows $E(4_1^+)$ against neutron number for a sizeable portion of the nuclear chart. While there are obvious trends, the data are anything but smooth and simple. For example, one can have a large factor difference of 4_1^+ energies for the same neutron number. However, suppose we plot $E(4_1^+)$, not against neutron number but against another collective observable, namely $E(2_1^+)$. Then the plot in Fig. 3(b) results. The difference in these two plots is striking. Figure 3(b) is very simple and compact. It shows two linear segments, one for high $E(2_1^+)$ values above about 100 keV, which has a least squares fitted slope of 2.00 ± 0.01, corresponding to an anharmonic vibrator satisfying, $E(4_1^+) = 2\ E(2_1^+) + a$, and one for low $E(2_1^+)$ values with a slope of 3.33 ± 0.01 with intercept near zero, corresponding to a deformed rotor. The figure shows a bi-partite classification of collective nuclei from Sr to Pb.

A final illustration of the value of bringing different perspectives to bear on a problem is provided by Figs. 4

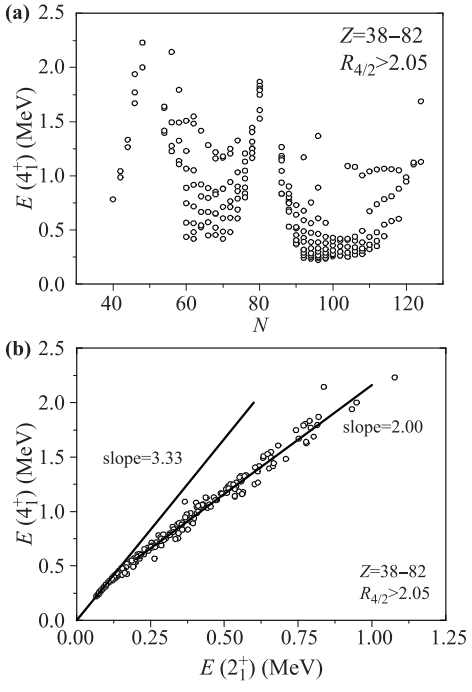

Fig. 3 $E(4_1^+)$ against neutron number **(a)** and against $E(2_1^+)$ **(b)** showing different perspectives on structural evolution. Based on Ref. [7].

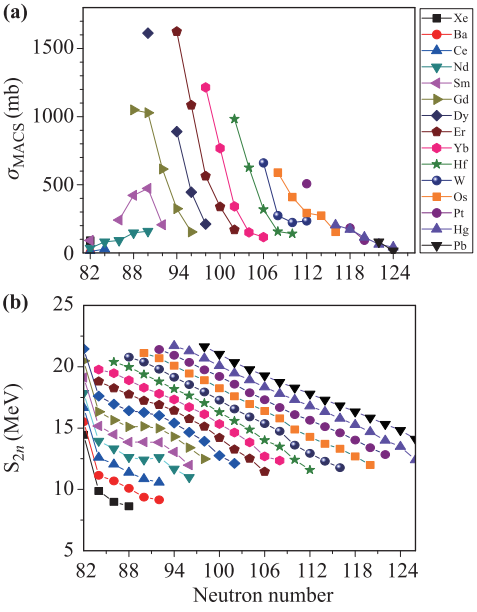

Fig. 4 **(a)** Maxwellian averaged 30 keV neutron capture cross sections in the rare earth region plotted against neutron number. **(b)** S_{2n}(N) values plotted against neutron number for the same region. Based on Ref. [11].

and 5. Neutron capture cross sections in the 10s of keV neutron energy regime are critical to understanding r-process nucleosynthesis. Results are needed for many nuclei for which data do not exist and for which such data are very difficult or impossible to obtain. Theory enters here and, for decades, many statistical model Hauser-Feshbach calculations have been done, with numerous degrees of freedom (and numerous parameters) to make such predictions. Yet different models can vary by an order of magnitude often only a few nucleons from stability. The empirical variations of these cross sections are illustrated in Fig. 4(a). Again, as with $E(4_1^+)$ against neutron number, there are some regularities but the figure likewise illustrates the difficulties of predicting cross sections for new nuclei.

Figure 4(b), though, hints at a different approach. It shows two nucleon separation energies against neutron number as well. Note that both plots are dominated by sequences of parallel trajectories.

It is thus interesting to plot the cross sections in a different way – instead of showing them against neutron number. Figure 5 shows the same cross sections plotted against $S_{2n}(N+2)$. The result is remarkable [11]. Now the neutron cross sections all lie of a compact smooth trajectory against $S_{2n}(N+2)$. The compactness, and the ability to fit these data with a simple smooth curve, allows one to predict cross sections to much higher accuracy, typically to within ±30%–40% even 5–10 masses beyond the last known points.

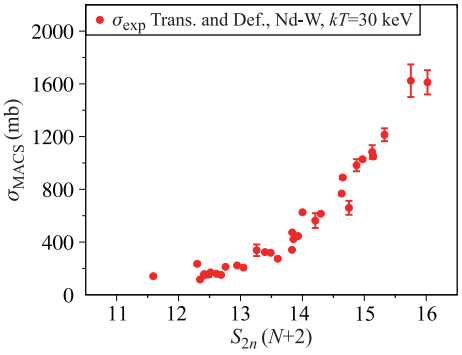

Fig. 5 Maxwellian averaged 30 keV neutron capture cross sections in the rare earth region plotted against $S_{2n}(N+2)$. Based on Ref. [11].

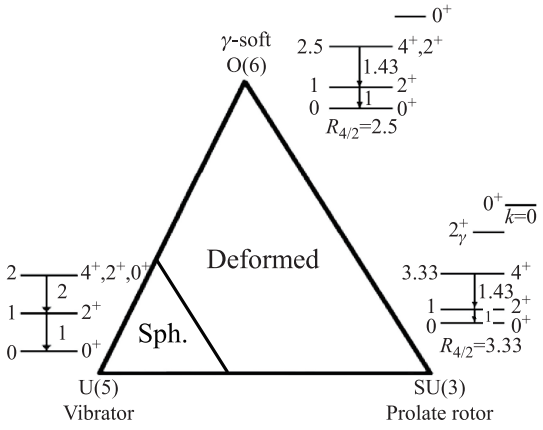

Fig. 6 Symmetry triangle of the IBA model showing the three dynamical symmetries at the vertices, the division into spherical and deformed regimes (Note that the locus and width of the transition region between these shapes is boson number-dependent). Each vertex gives the relevant $R_{4/2}$ value and the first few levels of a typical level scheme for that symmetry. Note that, except for U(5) and SU(3), $R_{4/2}$ does not uniquely define a position in the triangle but rather a contour or trajectory expressing a family of structures with that $R_{4/2}$. For example, $R_{4/2} = 2.5$ characterizes the O(6) limit, and a point along the U(5) to SU(3) leg, as well as a continuous arcing contour connecting these two points.

3 Symmetries and the evolution of structure

These simplicities and patterns reflect underlying order and, often, symmetries. Surely the most successful nuclear structure model embodying the idea of symmetries at play has been the IBA model with its dynamical symmetries, in which each step in a group chain invokes new quantum number(s), and additional degeneracy splitting according to those quantum numbers, new selection rules, and, often, analytic predictions for many observables. At the simplest level, the $R_{4/2}$ values of 2.0, 2.5 and 3.33 correspond to the U(5), O(6), and SU(3) symmetries and serve as a classification scheme for nuclear structure and its evolution. The idea is illustrated by the well-known symmetry triangle of Fig. 6. The model automatically makes a number of very general predictions. Examples are shown in Fig. 7(a) [7] for the evolution of structure along the line from the SU(3) to the O(6) symmetry, in terms of a single parameter χ (see below), for three observables (for a fixed boson number). One energy ratio, $E(2_2^+)/E(2_1^+)$, descends from infinity to around 2.0, another, for a $B(E2)$ branching ratio, trends oppositely, and a third, again a $B(E2)$ ratio, perhaps the most interesting, is zero in both symmetries and finite in between, reaching a maximum value near 0.07. These trends, which reflect the onset of axial asymmetry, provide several nice diagnostics. From the $E(2_2^+)/E(2_1^+)$ ratio one can extract the axial asymmetry variable γ. One can use the observable which vanishes in the two limits as an unambiguous signal for symmetry breaking, being non-zero only in between the symmetries. Particularly interesting are its actual values – never more than about 0.07. It is remarkable that this parameter-free result characterizes real nuclei almost exactly. For example, in the rare earth region this observable ranges from small values up to about 0.09 (in Os). This range is not input into the model but results from it and from the evolution of structure between the two symmetries.

While the structures behind these symmetries may sometimes seem obscure, they have a clear physical significance. The symmetry U(5) corresponds to a rather general spherical anharmonic vibrator characterized by quadrupole phonon and multi-phonon levels. Such structures are observed frequently near closed shells such as in the Cd nuclei (although admixed to some degree with two-particle-two hole cross shell proton intruder states). The symmetry SU(3) is a deformed symmetric rotor. The O(6) symmetry is that of a gamma-flat [$V(\gamma)$ is independent of γ] deformed rotor as first indicated in Refs. [12, 13].

The leg of the triangle from SU(3) to O(6) corresponds, in the IBA Hamiltonian, to the simple variation of a single parameter, χ, occurring in the form for the quadrupole operator as a function of s and d boson creation and destruction operators. Since SU(3) is axially symmetric (see below for a refinement of this idea) and O(6) is totally γ-flat, the variation of χ must correspond to a variation in an effective value perhaps best thought of as an average or rms value. One can make an interesting association of χ and γ by equating the values of the observables in Fig. 7(a) with those in a geometric model that is expressed in terms of the usual shape parameters β and γ. For this purpose we can use the Davydov model [14]. This model is not the geometric equivalent of the IBA since all axial asymmetry in the *s-d* IBA-1 model

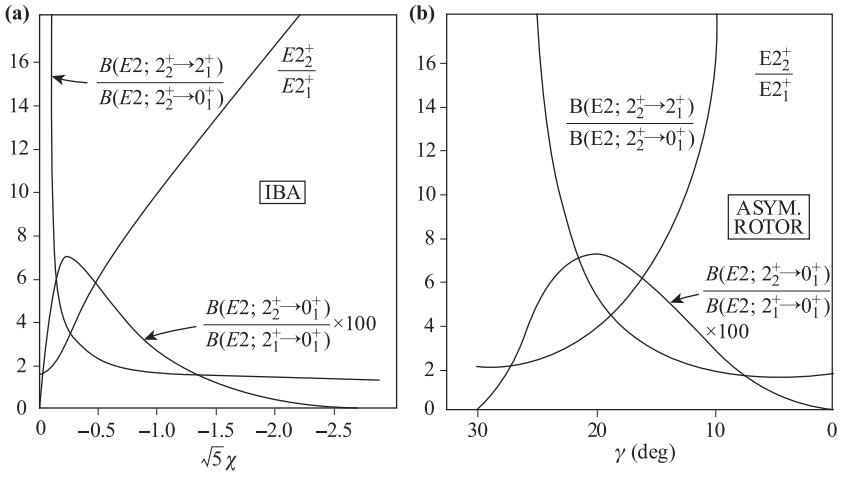

Fig. 7 **(a)** Three observables against the IBA parameter χ. **(b)** The same three observables calculated in the Davydov model [14] as a function of the axial asymmetry, γ. Based on Ref. [7].

arises from gamma softness, while $V(\gamma)$ in the Davydov has a sharp minimum at a specific γ value. Nevertheless, it is well-known that the values of nearly all observables for the ground state band and the low lying $K = 2$ vibration are nearly the same, in the two models, being sensitive only to the expectation value of γ. Hence, one can calculate the same observables in the Davydov model and relate them to the IBA model values. The results are shown in Fig. 7(b). It is remarkable how similar the general forms of the curves are.

Using these two panels one can make an association of any γ value with a corresponding χ value. Each observable gives a different correlation. If the correlations would be wildly different the concept of a γ–χ correlation would be invalid. But, as Fig. 8 shows, all three observables give very similar trajectories. Thus any IBA calculation along the important SU(3) to O(6) leg can be associated with a rather tightly constrained gamma value.

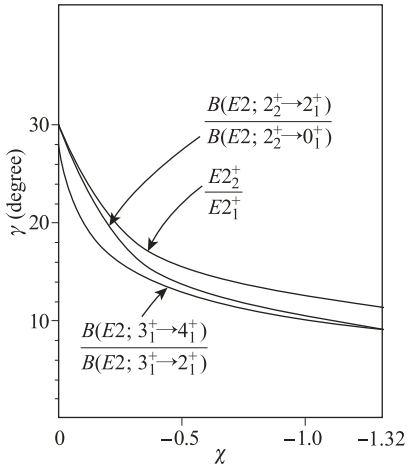

Fig. 8 The γ to χ relation determined for each of the observables in Fig. 7 by equating values of each observable. The reason the curves do not go to the axial limit on the right [towards SU(3)] is due to finite valence nucleon number leading to a potential soft against γ and the consequent zero point motion of the collective shape in that potential (see Fig. 9). Based on Ref. [7].

4 Finite valence nucleon number and the p-n interaction

One important and interesting caveat is appropriate here. Notice in Fig. 8 that γ does not go to zero in SU(3) as might be expected for an axially symmetric model. However, another key feature of the IBA that we have not discussed comes in here, namely its automatic inclusion of finite valence nucleon number effects since the total IBA Hamiltonian depends on boson number, N (half the total number of valence nucleons counted to the nearest closed shells). For finite N, the geometric potential, $V(\gamma)$, corresponding to an IBA Hamiltonian is not infinitely steep. There is therefore zero point motion which depends on N. These potentials are illustrated in Fig. 9. Because of the finite steepness, the expectation value of gamma will not go to zero even in SU(3) for finite N. The relation of the IBA to geometrical models has long been a subject of study. In addition to Refs. [1–7, 12, 13] see the pioneering paper in Ref. [15] where this is worked out in elegant detail.

The effects of finite N show up in many places in the corpus of IBA predictions. We will mention just one more.

In a geometric vibrator, the $E2$ operator consists simply of a quadrupole creation or destruction operator. Hence, an yrast B(E2) value of the form B(E2): $J \to J-2$, that is, from an N-phonon state to an $(N-1)$-phonon state is proportional to the phonon number in the initial states. Thus $B(E2 : 4^+ \to 2^+)/B(E2 : 2^+ \to 0^+) = 2$. In the IBA this is modified by the preservation of boson number in a given nucleus so that each destruc-

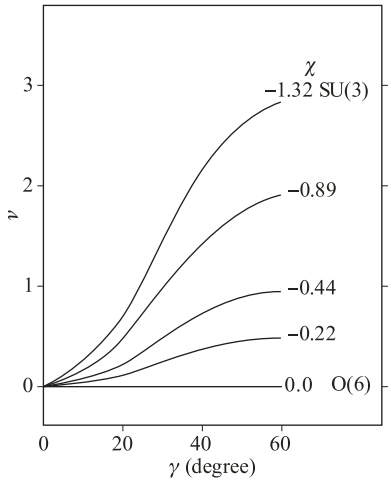

Fig. 9 The potential against γ in the IBA for $N = 16$ bosons and a variety of χ values from SU(3) to O(6). χ varies from -1.32 in SU(3) to 0 in O(6). Based on Ref. [7].

tion operator, d, must be accompanied by a corresponding creation operator, s^+. This gives an extra phonon number-dependent term in the $B(E2)$ value, and hence: $B(E2 : 4^+ \to 2^+)/B(E2 : 2^+ \to 0^+) = 2(N-1)/N$. For typical boson numbers for vibrational nuclei, say, 4, this gives $2 \times (3/4) = 1.5$. Hence the simplest application of the IBA to vibrational nuclei would predict that this ratio should scale roughly as 1.5.

In a geometric axial rotor the same $B(E2)$ ratio is given by the square of a ratio of Clebsch-Gordon coefficients, namely 1.43. In typical deformed nuclei the boson numbers are 12-16 and the effects of finite N on the predictions are intrinsically less, and hence the IBA predicts values of $B(E2 : 4^+ \to 2^+)/B(E2 : 2^+ \to 0^+)$ very close to 1.43 (typically about 1.4). Likewise, in O(6), the IBA predicts similar values as in SU(3). Perhaps unexpectedly, all three symmetries thus predict a very similar relation between these two B(E2) values, rather than an evolution from values near 2 to values near 1.4.

Thus we have the intriguing, and very robust, prediction that, almost independent of structure, the IBA predicts that $B(E2 : 4^+ \to 2^+) \sim 1.4$–$1.6\ B(E2 : 2^+ \to 0^+)$.

The data for all collective nuclei above about mass 100 are shown in Fig. 10. Remarkably, the data lie close to a straight line with slope 1.44. Normally one thinks of finite valence nucleon number effects as showing up at higher spin. Here we see a distinct example for the lowest yrast states.

There is another well known perspective where finite valence nucleon number is key, namely in the use of the N_pN_n scheme [16] and the P-factor [17]. These are defined, respectively, in terms of the numbers of valence protons, N_p, and the number of valence neutrons, N_n, simply as N_pN_n, and $P = N_pN_n/(N_p + N_n)$. The former is simply (twice) the number of p-n valence interactions while the latter can be thought of as the number of p-n interactions per pairing interaction. The idea behind these is that collectivity and deformation are largely driven by the p-n interaction among valence nucleons [18–21], in competition with the pairing interaction, which scales simply with the number of valence nucleons, and so the behavior of collective observables should have some smooth dependence on these quantities. This has been vetted and confirmed many times for many observables (see for example, [7, 16, 17]). Occasionally, a blind plot against these variables shows non-smooth behavior. Such deviations from the general behavior must point to a breakdown of the assumptions underlying these correlation schemes. In this case, they generally reflect changes in shell structure, and therefore in the counting of valence nucleons. We saw an example of this earlier in the context of Fig. 2 where $Z = 64$ functions as a mini-shell gap for $N = 82$–88 but disappears for $N = 90$ and larger. It was noted, but not discussed, that this was due to the monopole p-n interaction. In particular, it is the monopole p-n interactions between the protons in the $h_{11/2}$ orbit and the neutrons in the $h_{9/2}$ orbit as neutrons in the $N = 82$–126 shell first fill the $f_{7/2}$ orbit and then, near $N = 90$, the $h_{9/2}$ orbit. This orbit has high spatial overlap with the proton $h_{9/2}$ orbit and hence a strong interaction with it, which modifies the underlying single particle spectra, destroying the $Z \sim 64$ sub-shell gap. The onset of deformation with this mechanism was first proposed for the $A \sim 100$ region by Federmann and Pittel [20] and subsequently for the $A \sim 150$ region in Ref. [21].

Figure 11 illustrates a normal plot of a collective observable against nucleon number, showing high scatter and complex behavior, on the left and the corresponding simple, smooth N_pN_n plot on the right.

While we are discussing the valence p-n interaction, stressing that it depends on the spatial nature of the

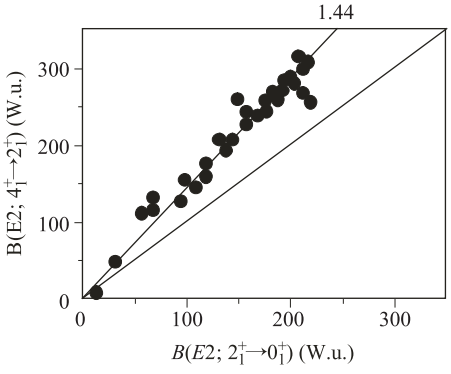

Fig. 10 Empirical $B(E2 : 4^+ \to 2^+)$ values plotted against $B(E2 : 2^+ \to 0^+)$ values for all collective nuclei ($R_{4/2} < 2.05$) from $Z = 38$–82. Based on Ref. [7].

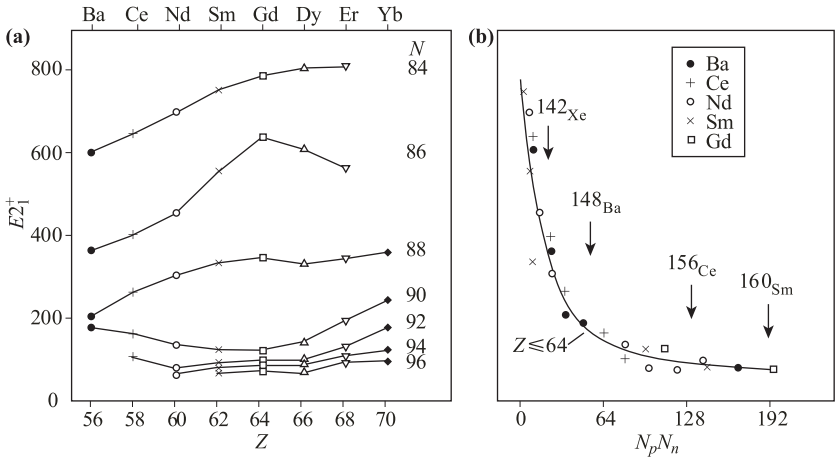

Fig. 11 **(a)** $E(2_1^+)$ againts proton number in the first half of the rare-earth region. Note the similarity to $R_{4/2}$ in Fig. 2 with, of course, the substitution of $R_{4/2}$ with $1/E2_1^+$. **(b)** The same data plotted against N_pN_n using the proton shell $Z = 50$–64 for $N < 90$ and $Z = 50$–82 for larger N. Based on Ref. [7].

proton and neutron orbits involved because the nuclear force is short range and attractive, it is interesting to mention a recent example. It is possible to extract empirical values of the p-n interaction of the last protons and neutrons, called δV_{pn}, from double differences of nuclear masses [22, 23]. The power of this approach has been shown extensively in Refs. [24–26] where it was found that basic collective observables, such as $R_{4/2}$, depend smoothly on δV_{pn}. Importantly, it was subsequently found [27] that δV_{pn} maximizes for a given element at the neutron number for which the respective proton and neutron Nilsson quantum numbers differ by $\Delta K[\Delta N, \Delta n_z, \Delta\Lambda] = 0[110]$ and that this occurs for $N_{val} \sim Z_{val}$ (an example in ^{168}Er with 18 valence protons and 18 valence neutrons–in this case, since one is looking at the filling of Nilsson orbits, one counts straight through the shell.). This difference, 0[110], in which the wave functions differ only by a single quantum in the z-direction, corresponds to very large spatial overlap. It was shown that the onset of deformation tracks very closely with the locus of $N_{val} \sim Z_{val}$.

We shall briefly return to mention the importance of the 0[110] difference in the next section when we talk about comparing different models with the data.

5 Comparing models

We have discussed looking at data from different perspectives. It is equally interesting to look at the data from the perspective of different models. In fact, one critique that can be made of some work in the field is that data are often compared only with a single model. Without seeing how other approaches fare, and (related concept) without considering theoretical uncertainties, it is risky to draw conclusions about structure from such singular comparisons. Here will illustrate this with one of the most iconic sets of observables in deformed nuclei, namely relative $B(E2)$ values from the decay of the collective vibrational γ-band to the ground band.

In the geometrical model of a perfect rigid rotor, that is, with clean separation of rotational and vibrational degrees of freedom, the ratio of $B(E2)$ values from a given level of the former band to the ground band are simply given by ratios of squares of Clebsch–Gordon coefficients. These are the well-known but sometimes overlooked Alaga rules [27]. For example (normalized to 100 for the denominator in each case):

1) $B(E2 : 2_\gamma^+ \to 0_g^+)/B(E2 : 2_\gamma^+ \to 2_g^+) = 70$

Similarly,

1) $B(E2 : 2_\gamma^+ \to 4_g^+)/B(E2 : 2_\gamma^+ \to 2_g^+) = 5$,

2) $B(E2 : 4_\gamma^+ \to 2_g^+)/B(E2 : 4_\gamma^+ \to 4_g^+) = 34$,

3) $B(E2 : 5_\gamma^+ \to 4_g^+)/B(E2 : 5_\gamma^+ \to 6_g^+) = 57.1$.

Given the utter simplicity of these predictions, depending on nothing other than the separation of rotational and intrinsic degrees of freedom (hence the goodness of the K quantum number) these simple, analytic, parameter-free predictions are surprisingly good. Who would expect that detailed properties of subtle transition rates connecting states of different intrinsic structure in complex nuclei with up to hundreds of nucleons of two types, interacting with the electromagnetic and strong forces coulld be so easily predicted.

Despite what is truly an impressive accord, there are undeniable deviations, that grow with spin. Furthermore, they exhibit other regularities. The most obvious is that transitions the *decrease* spin are always less than the Alaga rules and those that *increase* the spin are always greater than the Alaga rules. Furthermore, though not obvious from what we show here, the deviations are least near mid-shell and largest at the edge of the deformed region where the separation of rotational and vibrational degrees of freedom is least good.

A systematic set of deviations this regular suggests a simple origin. Indeed, since the 1960's there has been a standard explanation, namely the invocation of bandmixing between the γ and ground bands, as discussed in pioneering papers by Lipas [29] and Riedinger *et al.* [30]. Owing to the nature of the raising operators inducing this mixing, the effects automatically grow with spin, in accord with the data, and have the spin increasing and decreasing behavior noted experimentally. In fact, it is rather easy to extract, for any given nucleus, a single bandmixing parameter, related to the strength of the mixing matrix element, that usually accounts remarkably well for the data. This parameter, called Z_γ, for example is ~0.035 for ^{168}Er. A full comparison of the data, the Alaga rules and a bandmixing calculation are shown for this nucleus in Table 1. It is clear that one obtains exceptionally good agreement for all the data with a single parameter.

But, when one encounters a successful model (Alaga plus bandmixing in this case), it is always useful to delve deeper and try to understand the physics origin. In this context it is worth noting that the mixing amplitudes required to reach agreement with the B(E2) data are extraordinarily small. They are typically <0.01 for low spins. The reason they can affect B(E2) values by significant percentages is simple: In effect, they admix amplitudes of very large intraband matrix elements, e.g., $2_1^+ \rightarrow 0_1^+$, albeit with small amplitudes, into very weak interband matrix elements, e.g. $2_\gamma^+ \rightarrow 0_1^+$.

Given the above results, it is appropriate to ask if there are other models that can reproduce the same data and if they do so by virtue of the same implicit physics. In one case, this was answered affirmatively decades ago, when one-parameter IBA calculations (using the CQF approach [7, 31]) were carried out. The results of the IBA calculations are included in Table 1 and the agreement, both with the data and the bandmixing calculations, is spectacular.

Trying to understand this concordance of predictions, resulting from a geometrical model and from a model couched in terms of two-particle entities called s and d bosons may not seem easy but in fact is well understood. Recall, Fig. 8 which showed the relation between the IBA parameter, χ, and the deformation variable, γ. The one parameter in the CQF calculations in Table 1 is indeed χ, Hence the IBA calculations are equivalent to introducing a finite axial asymmetry and it is well known that bandmixing and axial asymmetry are intimately linked, as can be seen by the changes in interband B(E2) values in the Davydov model as a function of γ, which closely mimic those of the bandmixing model as a function of γ.

Now, however, we turn to two other models that give predictions, shown in Table 1 as well, that have an interesting relation to our discussion. The first is called PDS, for Partial Dynamical Symmetry [32], and is an offshoot of the IBA model in which certain states have a pure symmetry and others break that symmetry. In the particular case at hand, we are dealing with an SU(3)-PDS, in which the γ and ground bands are absolutely pure SU(3) and other bands break SU(3) with various mixing matrix elements. These PDS predictions are included in Table 1 and show an interesting relation to the data and the Alaga rules. They display exactly the same *patterns* of deviations from the Alaga rules, in accord with the data, but the deviations from the Alaga rules are only about half those required to match the data.

Table 1 Relative $B(E2)$ values from given states in the γ-band to multiple states in the ground band in ^{168}Er compared to the following theoretical predictions in successive columns: The parameter-free Alaga rules; a one parameter bandmixing approach; a one parameter IBA model in the Consistent Q formalism [31]; the parameter-free SU(3) partial dynamical symmetry (PDS) (see Ref. [32]); and the parameter-free approximate Proxy-SU(3) symmetry [33–35].

$J_{initial}$	J_{final}	^{168}Er-EXP	ALAGA	$Z_{gamma} = 0.035$	IBA(CQF)	PDS	PROXY
2_γ	0^+	56.2(11)	70	56.9	54	64.3	52.9
	2^+	100	100	100	100	100	100
	4^+	7.3(4)	5	7.6	8	6.3	8.5
3_γ	2^+	100	100	100	100	100	100
	4^+	62.6(14)	40	62.9	69	49.3	73
4_γ	2^+	19.3(4)	34	20.2	18	28.1	16.4
	4^+	100	100	100	100	100	100
	6^+	13.1(12)	8.6	16	16	12.5	18.7
5_γ	4^+	100	100	100	100	100	100
	6^+	123(14)	57.1	117	125	79.6	147.7
6_γ	4^+	11.2(10)	26.9	11	9	20.3	7.4
	6^+	100	100	100	100	100	100
	8^+	37.6(72)	10.6	23.6	20	18	27.9

By definition, the PDS does not involve any bandmixing. The deviations from the Alaga rules are related to finite boson number effects. Yet, somehow, not yet fully understood, they produce very similar results. Regardless of the underlying reason, one possible interpretation could be that, if one accepts the PDS starting point and adds bandmixing effects on to it, that the real mixing in actual nuclei is only a half of what has been thought for half a century. That is, in this view, the deviations of the data from the Alaga rules would be partly due to an intrinsic property of the PDS and to about half the mixing previously thought needed. Or, there could be some other interpretation. Until we understand this, it is hard to look at the successful bandmixing or IBA-CQF calculations as giving the definitive physics. Maybe they do, or maybe the PDS is telling us something different. It is only by having compared this model as well that we are even made aware of the possibility of an alternate understanding.

The final example of a model for these same data is a new approach called the Proxy-SU(3) model [33, 34]. This is not the place to discuss it in any detail. We only note that it is based on an attempt to recover a fermionic SU(3) model for heavy nuclei where normal SU(3) is badly broken by the intruder unique parity orbit which descends into the shell below (e.g., the proton $h_{11/2}$ orbit into the $Z = 50$–82 shell). This results in single particle sequences between magic numbers that do not satisfy the requirements of SU(3)-namely a full set of orbits with orbital angular momentum $0, 2, 4, \ldots$ (or, $1, 3, 5, \ldots$) with both $j = l + 1/2$ and $j = l - 1/2$ states.

There have been numerous attempts to recover an SU(3) symmetry. The most well-known is, of course, pseudo-SU(3) [36]. Proxy-SU(3) uses a different approximate orbit substitution, inspired by the above-mentioned importance of spatial overlaps in Nilsson orbits whose quantum numbers differ by 0[110]. The result is a set of parameter-free predictions of the deformation parameters β and γ, which agree very well with the data in the rare earth region. Using the effective γ values, one can then use the Davydov model to predict relative B(E2) values, which are shown in Table 1 under the heading Proxy. It is seen that they too give deviations from the Alaga rules, again, in the correct directions as given by the data, and that these parameter-free predictions are in nearly as good agreement with the data as the bandmixing or IBA predictions and are comparable to the PDS predictions.

The point of this entire section is that one can learn a lot by comparing multiple models with the same data. In the present example, one model contains nothing more than a complete separation of rotational and intrinsic degrees of freedom, another introduces bandmixing in a geometrical framework, another does so in an algebraic, symmetry-based approach, another avoids mixing altogether but still does reasonably well, and a final approach is based on an approximation to the shell model in heavy nuclei.

The fact that all these approaches work is, in itself, fascinating. It raises questions as to the relations of these models, and, most importantly, it highlights the value of multiple approaches to understanding the structure of atomic nuclei. If there is a simple message here, it is that one should not simply pick one's favorite model and compare it in isolation to a given set of data.

6 Summary

We have looked at the structure of nuclei from a number of synthetic ways, emphasizing the value of viewing the data from multiple perspectives, the beautiful regularities and patterns that nuclei exhibit, the remarkable role of (dynamical) symmetries, the importance of valence p-n interactions, and the value of interpreting nuclear data with a variety of model approaches.

Acknowledgements I am profoundly grateful to Akito Arima and Franco Iachello for the physics they have introduced to understand nuclei, for the inspiration they have provided, and for their guidance and counsel over more than 4 decades. I am so thankful to R. Burcu Cakirli for her friendship and for the wonderful collaborative work we have done throughout the third millennium, much of which is reflected in these pages, and to D. D. Warner, N. V. Zamfir, P. von Brentano, J. Jolie, W. Nazarewicz, B. S. Sherrill, H.B. Borner, I. Talmi, D. Bonatsos, K. Heyde, P. Van Isacker, A. Couture, K. Blaum, N. Pietralla, S. Pittel, A. Macchiavelli, V. Werner, D. S. Brenner, A. Leviatan, L. L. Riedinger, E. A. McCutchan, J. A. Cizewski, A. Aprahamian, R. V. Jolos, A. Frank, O. Scholten, D. A. Bromley for so many collaborations, discussions, insights, and support over the years. I am sure I have forgotten others and to them I apologize.

References and notes

1. A. Arima and F. Iachello, New symmetry in the *sd* boson model of nuclei: The group $O(6)$, *Phys. Rev. Lett.* 40, 385 (1978)
2. A. Arima and F. Iachello, Interacting boson model of collective states (I): The vibrational limit, *Ann. Phys.* 99, 253 (1976)
3. A. Arima and F. Iachello, Interacting boson model of collective nuclear states (II): The rotational limit, *Ann. Phys.* 111, 201 (1978)
4. A. Arima and F. Iachello, Interacting Boson model of collective nuclear states (IV): The $O(6)$ limit, *Ann. Phys.* 123, 468 (1979)

5. A. Arima, T. Otsuka, F. Iachello, and I. Talmi, Collective nuclear states as symmetric couplings of proton and neutron excitations, *Phys. Lett. B* 66, 205 (1977)
6. D. R. Janssen, R. V. Jolos, and F. Donau, An algebraic treatment of the nuclear quadrupole degree of freedom, *Nucl. Phys. A* 224, 93 (1974)
7. R. F. Casten, Nuclear Structure from a Simple Perspective, 2nd Ed., Oxford University Press, 2000
8. R. B. Cakirli and R. F. Casten, Empirical signature for shape transitions mediated by sub-shell changes, *Phys. Rev. C* 78, 041301(R) (2008)
9. R. F. Casten and N. V. Zamfir, Empirical realization of a critical point description in atomic nuclei, *Phys. Rev. Lett.* 87, 052503 (2001)
10. F. Iachello, Analytic description of critical point nuclei in a spherical-axially deformed shape phase transition, *Phys. Rev. Lett.* 87, 052502 (2001)
11. A. Couture, R. F. Casten, and R. B. Cakirli, Simple, empirical approach to predict neutron capture cross sections from nuclear masses, *Phys. Rev. C* 96, 061601(R) (2017)
12. J. A. Cizewski, R. F. Casten, G. J. Smith, M. L. Stelts, W. R. Kane, H. G. Borner, and W. F. Davidson, Evidence for a new symmetry in nuclei: The structure of ^{196}Pt and the $O(6)$ limit, *Phys. Rev. Lett.* 40, 167 (1978)
13. R. F. Casten, Interacting Bosons in Nuclear Physics, Ed. F. Iachello, Plenum Press, New York, 1978, p. 37
14. A. S. Davydov and G. F. Filippov, Rotational states in even atomic nuclei, *Nucl. Phys.* 8, 237 (1958)
15. J. N. Ginocchio and M. W. Kirson, An intrinsic state for the interacting boson model and its relationship to the Bohr–Mottelson model, *Nucl. Phys. A* 350(1–2), 31 (1980)
16. R. F. Casten, N_pN_n systematics in heavy nuclei, *Nucl. Phys. A* 443(1), 1 (1985)
17. R. F. Casten, D. S. Brenner, and P. E. Haustein, Valence p-n interactions and the development of collectivity in heavy nuclei, *Phys. Rev. Lett.* 58(7), 658 (1987)
18. A. de-Shalit and M. Goldhaber, Mixed configurations in nuclei, *Phys. Rev.* 92(5), 1211 (1953)
19. I. Talmi, Effective interactions and coupling schemes in nuclei, *Rev. Mod. Phys.* 34(4), 704 (1962)
20. P. Federman and S. Pittel, Towards a unified microscopic description of nuclear deformation, *Phys. Lett. B* 69(4), 385 (1977)
21. R. F. Casten, D. D. Warner, D. S. Brenner, and R. L. Gill, Relation between the $Z = 64$ shell closure and the onset of deformation at $N = 88$–90, *Phys. Rev. Lett.* 47(20), 1433 (1981)
22. J. D. Garrett and Z.Y. Zhang, Abstract, International Conference on Contemporary Topics in Nuclear Structure Physics, Cocoyoc, Mexico, June 9–14, 1988
23. J. Y. Zhang, R. F. Casten, and D. S. Brenner, Empirical proton-neutron interaction energies: Linearity and saturation phenomena, *Phys. Lett. B* 227(1), 1 (1989)
24. R. B. Cakirli, D. S. Brenner, R. F. Casten, and E. A. Millman, Proton-neutron interactions and the new atomic masses, *Phys. Rev. Lett.* 94(9), 092501 (2005) [Erratum: *Phys. Rev. Lett.* 95(11), 119903 (2005)]
25. D. S. Brenner, R. B. Cakirli, and R. F. Casten, Valence proton-neutron interactions throughout the mass surface, *Phys. Rev. C* 73(3), 034315 (2006)
26. R. B. Cakirli and R. F. Casten, Direct empirical correlation between proton-neutron interaction strengths and the growth of collectivity in nuclei, *Phys. Rev. Lett.* 96(13), 132501 (2006)
27. R. B. Cakirli, K. Blaum, and R. F. Casten, Indication of a *mini-valence* Wigner-like energy in heavy nuclei, *Phys. Rev. C* 82, 061304(R) (2010)
28. G. Alaga, K. Alder, A. Bohr, and B. R. Mottelson, Intensity rules for beta and gamma transitions to nuclear rotational states, *Dan. Mat. Fys. Medd.* 29, 9 (1955)
29. P. O. Lipas, Perturbation corrections to energies of collective states in deformed even nuclei, *Nucl. Phys.* 39, 468 (1962)
30. L. L. Riedinger, N. R. Johnson, and J. H. Hamilton, β- and γ-Vibrational Bands of ^{152}Sm and ^{154}Gd, *Phys. Rev.* 179(4), 1214 (1969)
31. D. D. Warner and R. F. Casten, Revised formulation of the phenomenological interacting boson approximation, *Phys. Rev. Lett.* 48(20), 1385 (1982)
32. A. Leviatan, Partial dynamical symmetry in deformed nuclei, *Phys. Rev. Lett.* 77(5), 818 (1996)
33. D. Bonatsos, I. E. Assimakis, N. Minkov, A. Martinou, R. B. Cakirli, R. F. Casten, and K. Blaum, Proxy-$SU(3)$ symmetry in heavy deformed nuclei, *Phys. Rev. C* 95, 064325 (2017)
34. D. Bonatsos, I. E. Assimakis, N. Minkov, A. Martinou, S. Sarantopoulou, R. B. Cakirli, R. F. Casten, and K. Blaum, Analytic predictions for nuclear shapes, prolate dominance, and the prolate-oblate shape transition in the proxy-$SU(3)$ model, *Phys. Rev. C* 95, 064326 (2017)
35. Talks by R. F. Casten and R. B. Cakirli to be given at SSNET18, Nov. 5–9, 2018, Paris, France
36. R. D. Ratna Raju, J. P. Draayer, and K. T. Hecht, Search for a coupling scheme in heavy deformed nuclei: The pseudo $SU(3)$ model, *Nucl. Phys. A* 202(3), 433 (1973)